Roughness-induced instability in stripe domain patterns

Joo-Von Kim, M. Demand, Michel Hehn, K. Ounadjela, R. Stamps

Roughness-induced instability in stripe domain patterns

Joo-Von Kim,[1] M. Demand,[2,*] M. Hehn,[3] K. Ounadjela,[2] and R. L. Stamps[1]
[1]*Department of Physics, The University of Western Australia, Nedlands WA 6907, Australia*
[2]*IPCMS, 23 rue du Loess, 67037 Strasbourg Cedex, France*
[3]*Laboratoire de Physique des Matériaux, UMR CNRS 7556, 54506 Vandoeuvre les Nancy Cedex, France*
(Received 27 December 1999)

Island dominated growth in cobalt/ruthenium structures is used to create films with varying degrees of structural roughness. The resulting magnetic films constructed in this way are continuous thin films with a distribution of islands on the surface. The size and spacing of the islands are remarkably uniform, and the degree of roughness is determined by varying the thickness of the continuous film relative to the density and size of the islands. The evolution of coercive fields, saturation fields and remanence are studied for differing degrees of roughness, and particular attention is given to consequent effects on domain pattern formation and stability. The stability of the stripe domain pattern is sensitive to the island structure, and strong correlations are found between domain pattern stability and film structure. Two types of behavior are found and the transition region between these behaviors is studied experimentally and theoretically in terms of stability to effects of roughness. A scheme to distinguish between randomly and regularly distributed defects based on measuring stripe domain quality is suggested.

I. INTRODUCTION

A wide variety of two and three dimensional systems exhibit equilibrium patterned structures in the form of bubbles and stripes.[1] Examples include Langmuir monolayers,[2] ferrofluid films,[3] and magnetic garnets.[4] Such systems allow studies of the stability of the domain structures versus external perturbations[5,6] and classification according to phase diagrams and transitions.[7]

The dynamics of pattern structures is a fascinating and difficult topic because the systems under study are far from equilibrium, and governed by highly nonlinear interactions. Magnetic systems are very useful for this purpose because of the ease with which domain patterns can be constructed and studied. An example of work performed on these kind of questions is a study of magnetic garnets using an Ising model based analysis.[8] The formation and stability of magnetic domain patterns is also a particularly important issue for applications to magnetic recording technologies. In this context, key questions involve the stability of domains relative to various effects associated with film and device fabrication. One of the most difficult issues is the effects of imperfections and roughness on domain pattern formation and stability. Roughness enters in a variety of ways, influencing the nucleation and pinning of domain boundary walls, as well as affecting magnetic ordering within domains. A critical problem is an accurate and meaningful way of quantifying roughness in terms of relevant effects.

A model experimental system is investigated in this paper in which roughness is induced via controlled island growth in a continuous magnetic film. The magnetic island growth is determined by the structure of an underlying ruthenium buffer layer. As shown in a previous paper,[9] there is an ''optimum'' Ru thickness where a narrow size distribution of well separated islands are formed. The Ru buffer is used as a basis for further cobalt growth, and results in several stages, or regimes, of Co island and film growth. The last stage is one described as a continuous Co film supporting a network of islands.

The investigations of this paper are primarily concerned with structures in this latter regime. In particular, the consequent effects on magnetic properties, with particular attention to stripe domain pattern formation, are examined as the degree of island formation is changed. The degree of island formation is essentially inversely proportional to the thickness. Two different thickness regions are found which can be used to characterize the magnetic properties. Films with thicknesses above a critical value support a well defined perpendicular stripe domain pattern and have hysteresis loops with coercive fields and nucleation fields typical of a continuous magnetic film. The other region occurs for thicknesses below this critical value and is characterized by wandering domain walls which are only weakly oriented out of plane. The magnetic hysteresis is also atypical of continuous films, and the transition is identified as the point at which the roughness dominates the magnetic properties of the film.

The paper is organized as follows: In Sec. II, the physical and magnetic properties of the films are discussed. In Sec. III, stability of stripe domain patterns to perturbations induced by film roughness is described. A method of quantifying the quality of the stripe patterns is presented, and numerical simulations are used to interpret the experimental results. The conclusions are summarized in Sec. IV.

II. FILM GROWTH AND CHARACTERIZATION

A. Film preparation

A detailed description of the growth conditions and structure of the films is given elsewhere,[9] so only the important details are reported here. The emphasis of the previous work was on films with relatively little Co coverage, while the present work focuses on thicker Co films which display very different magnetic properties.

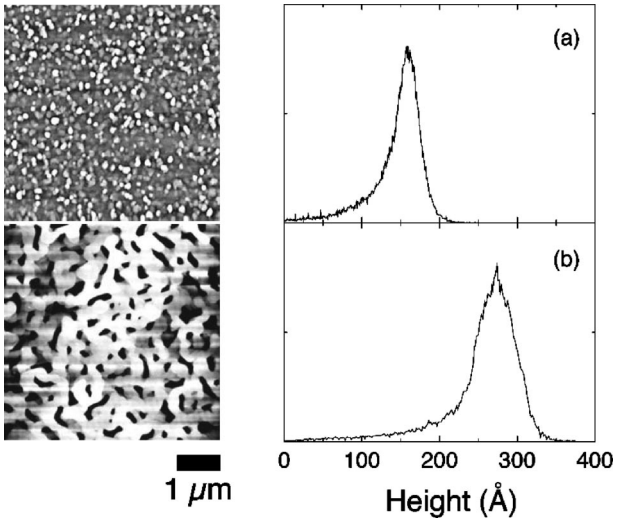

FIG. 1. Surface profile characterization of Co films grown on Ru. The Co film thickness are (a) $t_{Co}=200$ Å and (b) $t_{Co}=600$ Å. The dimensions of each AFM image is 5 μm$\times$5 μm. The left panels are AFM gray scale images, and the right panels are the corresponding height distributions.

The films were grown by first depositing a Ru layer at 700 °C on mica. The nominal thickness for the Ru was set at 50 Å since it was determined that this produced a narrow distribution of uniformly spaced Ru islands with a mean height of 60 Å. The structure is hcp(0001) and the island lateral size ranges between 200 and 300 Å. This island structure serves as a base for subsequent Co growth.

The Co was deposited at 500 °C and capped with 30 Å Ru. A range of Co thicknesses was examined, from 45 Å to 1000 Å. Samples with Co thicknesses below 150 Å are primarily unconnected Co islands, whereas for thicknesses greater than 150 Å, the islands appear to be superimposed on an underlying continuous film structure. The magnetic properties of the thin film regime are those of independent magnetic particles and were discussed previously.[9] Here the discussion concerns samples with thicknesses between 200 Å and 1000 Å and that behave magnetically like continuous, though imperfect, thin films.

An idea of the structure can be ascertained from atomic force microscopy (AFM) images on the samples. An example is shown in Fig. 1 where AFM images for (a) a 200 Å Co film, and (b) a 600 Å Co film are shown. The accompanying panels on the right show the height distribution determined from the AFM scan. The distribution is sharply peaked at 160 Å for the 200 Å film and at 270 Å for the 600 Å film. The width of the height distribution is roughly 100 Å in both cases.

The panels on the left in Fig. 1 are gray scale images determined from the AFM scan. The 200 Å film appears as a collection of isolated islands whereas the 600 Å film is more of a collection of overlapping islands separated by small gaps. All the films are believed to be composed of a Co island network with an underlying continuous Co film component. The island network appears to have two different structures as well. The structure for the 200 Å thick Co is that of a continuous film surrounded by islands. The structure for films above 600 Å is more that of islands with ridges surrounding many deep valleys in the Co. The 600 Å film is believed to be in a crossover region between an island dominated film and a continuous Co film. The significance of this for the magnetic properties will be discussed in Sec. IV.

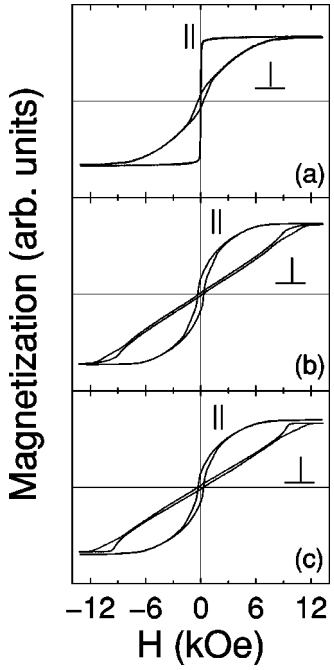

FIG. 2. Parallel and perpendicular magnetization curves performed at room temperature for (a) $t_{Co}=200$ Å, (b) $t_{Co}=600$ Å, and (c) $t_{Co}=760$ Å.

B. Hysteresis loops

Magnetic hysteresis is shown in Fig. 2 where magnetization measurements are shown for the 200, 600, and 760 Å films. Results for field aligned parallel and perpendicular to the film plane are shown. The perpendicular magnetization curve measured on the thinnest film in Fig. 2(a) shows an important hysteresis at low field which is characteristic of a Co film having a planar and a perpendicular component of the magnetization. Indeed the magnetization curves for Co thicknesses below 500 Å are characteristic of a weak-stripe regime. This regime has been observed for smooth Co films by Hehn *et al.*[10] and Donnet *et al.*[11] The shapes of both the parallel and perpendicular hysteresis for the thicker films are identical to those obtained on high quality smooth epitaxial Co films.[10] The evolution of the hysteresis with increasing film thickness provides information about the ability to nucleate domain walls and also the stability of domain patterns.

Quantitative measures of the ability to nucleate domains and domain stability can be obtained from the hysteresis curve. Characteristic points are plotted in Fig. 3 as functions of Co thickness. The points are the coercive field H_c, the saturation field H_s, and the remanence M_r. The coercive field is defined as the half-width of the hysteresis loop. For a symmetric loop centered about $H=0$, it is defined as $M(H_c)=0$. The saturation field is the field at which the magnetization attains its saturation value M_s, i.e., $M(H_s)=M_s$. The remanence is the magnitude of magnetization at zero field, i.e., $M(0)=M_r$. The curves show little variation in these quantities for Co film thicknesses above 600 Å. This

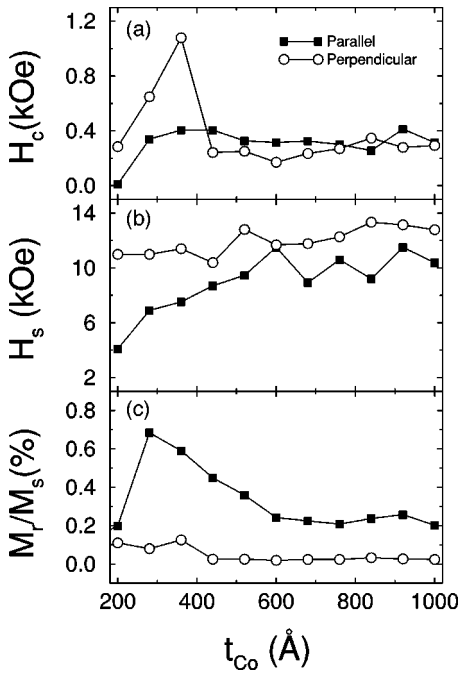

FIG. 3. Behavior of the (a) parallel and perpendicular coercive field H_c, (b) saturation field H_s, and (c) remanent magnetization M_r as functions of nominal cobalt thickness.

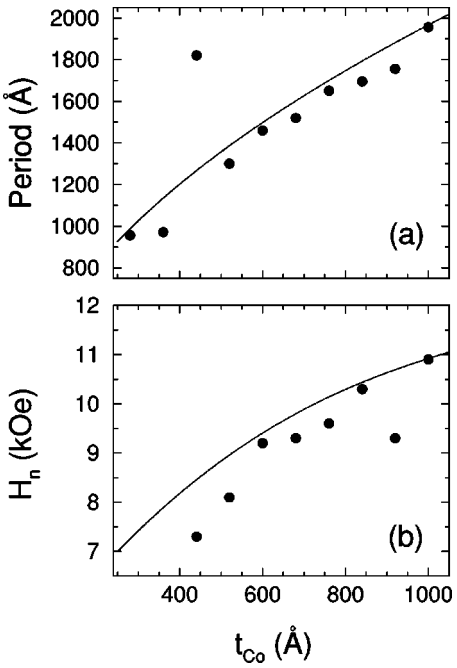

FIG. 4. (a) Domain period versus nominal cobalt thickness, and (b) nucleation field versus nominal cobalt thickness. The open circles are experimental data points and the lines are calculated curves. Above 600 Å Co thickness, the period shows a steady increase in agreement with calculation.

is particularly true for the coercive field and remanence, whereas the saturation field shows somewhat larger fluctuations. The coercive field is small, around 300 Oe. Both parallel and perpendicular saturation fields increase slightly with increasing Co thickness as observed for smooth cobalt films[10] and the evolution versus thickness can be calculated for thicknesses above 40 Å.[12,13]

Below 600 Å, all quantities show large, in some cases systematic, deviations from thick film behavior. The coercive fields and remanence show the largest deviations. The magnitude of the deviations for films between 200 and 600 Å is roughly 1 kOe for the coercive field, and less than 1.0% for the remanence. The saturation field in the parallel configuration shows a steady decrease with decreasing thickness, ranging from 10 kOe at 600 Å to 4 kOe at 200 Å. The coercive field for parallel magnetization also shows a steady decrease over this thickness range, ranging from 300 Oe at 600 Å to zero at 200 Å. A trend also exists in the remanence showing an increase as the thickness decreases from 600 Å, except for the 200 Å film which has a low remanence.

C. Domain formation

The parallel field hysteresis shows increases in remanence, decreases in saturation, and reduced coercivity for thicknesses below 600 Å compared to thicknesses above 600 Å. These changes are consistent with a magnetization process controlled by domain wall nucleation and domain pattern formation. Perpendicular stripe domains are formed for the thickest films, and the thin films support stripe domains where the magnetization is only partly oriented perpendicular to the film. In general, the spacing between domain walls increases with increasing film thickness. The corresponding qualitative effect on the hysteresis curves is a broadening of the parallel and perpendicular magnetization loops and appearance of minor loops in the perpendicular measurement for the films with thicknesses above 500 Å. Those minor loops are characteristic of the formation of domains with perpendicular magnetization.[14] This is fully consistent with the observed trends in the coercivity fields and remanence.

The stripe domain patterns formed in the thicker films are very narrow, and magnetic force microscopy (MFM) shows that the spacing in these films can be within an order of magnitude of the domain wall width for the thinnest films. The width of a domain wall is approximately $\pi\sqrt{A/K}$, where A is the exchange stiffness of the material and K is the anisotropy energy. For cobalt, the domain wall width is calculated to be approximately 170 Å. This trend is shown in Fig. 4(a) where the period of the domain stripe period is shown as a function of Co thickness. Above 500 Å Co thickness, the period shows a steady increase and in fact agrees well with a calculation of the period for a periodic stripe pattern with perpendicular magnetization in a smooth, continuous film.[10,14] Below 600 Å Co thickness, the data shows some deviations from the expected behavior because the magnetization is not fully perpendicular to the film plane, but canted.

The regularity of the stripe patterns will be discussed in detail later, and for the moment it is important to note only that some aspects of regularity in the patterns improve with increasing Co film thickness. A signature of this is the development of a sharp, well defined nucleation field characteristic of a smooth thin film. The nucleation field becomes most pronounced for Co film thicknesses above approximately 600 Å. Below 600 Å, the islanding appears to strongly affect the domain wall and pattern formation process. This is not surprising since surface imperfections can act as nucleation centers with a distribution of nucleation

fields and volumes. The shape of the minor loops near saturation in Fig. 2 show how the nucleation field becomes better defined as the Co thickness is increased. This is consistent with the idea that the roughness becomes less important as the film becomes thicker.

The calculated and measured nucleation fields are given in Fig. 4(b). The determination of a nucleation field from the hysteresis curve is somewhat ambiguous as it is difficult to identify a single clear field at which nucleation can be said to begin. As shown in Fig. 2, the thinnest films have very rounded minor loops where nucleation takes place, indicating a large distribution of nucleation fields. This can be expected as the roughness becomes more important relative to the continuous film behavior by providing more avenues for domain wall formation at different applied field strengths. The nucleation fields as a function of Co film thickness were also calculated using Thiele's model,[13] and shown by the solid line in Fig. 4(b). In Thiele's model, the quantity $K/(2\pi M_s^2)$ is assumed to be infinite (or at least very large), where K is the anisotropy energy and M_s is the saturation magnetization. For Co films this quantity is not small, and good fits can be still achieved for smooth films. There is reasonable agreement with the expected value for thicknesses above 500 Å, and the general trend seems to be followed for thicknesses below 500 Å (in so far as a nucleation field can be identified).

In summary, the stripe period and domain nucleation field measurements extend previous measurements on these kinds of films into a thickness range below 1000 Å thickness.[10] Two distinct regions have been identified for the magnetic properties in relation to the Co film thickness. Above 500 Å Co film thickness, the magnetization processes are typical of smooth, continuous Co films controlled by the formation of perpendicular stripe domains. Below 600 Å, the magnetization process is again controlled by the formation of stripe domains, but the nucleation and coercivity fields appear to deviate from those of a comparable thickness smooth film with perpendicular magnetization. A transition between these two regions occurs around 500 Å Co thickness.

We note that the behavior above and below the film thickness of 600 Å may be due to a difference in the domain magnetization orientation. The domain patterns are perpendicularly oriented for thicknesses above 600 Å, but for thicknesses less than 600 Å, the magnetization is weakly in-plane oriented.

III. DOMAIN PATTERN STABILITY

The quality of the parallel stripe domain patterns is now discussed. The idea is motivated by noting that the magnetic properties become strongly affected by the islanding as the film thickness is decreased below 600 Å, though aspects of the continuous film properties are retained. This is no longer true below 200 Å Co film thickness,[15] where the magnetic properties appear to be more those of separate Co islands than those of a continuous Co film. The remainder of the paper is devoted to a discussion of how the stripe domain pattern can signal a transition between strongly interacting island behavior and continuous film behavior.

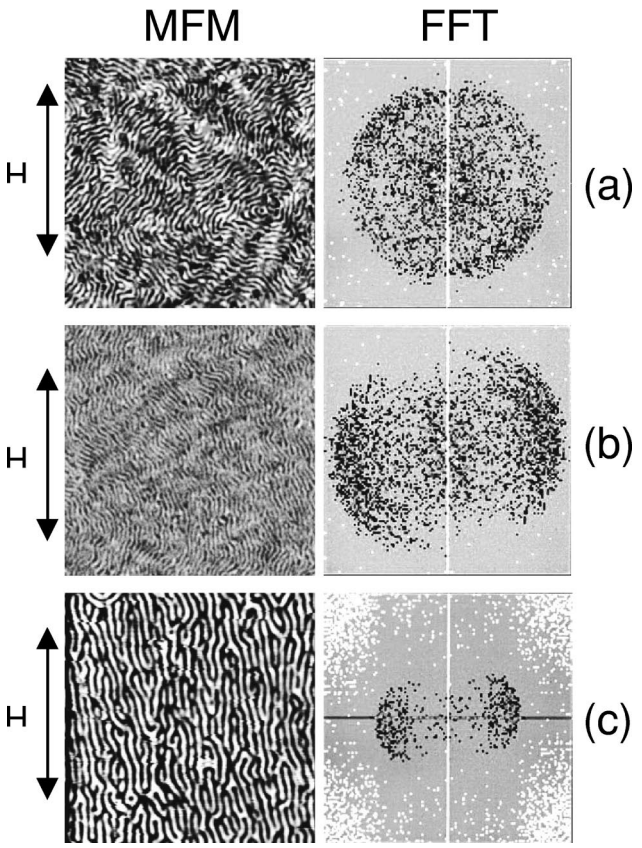

FIG. 5. 5 μm$\times$5 μm MFM images after parallel demagnetization (left) and the corresponding two-dimensional Fourier transforms (right) for (a) $t_{Co}=200$ Å, (b) $t_{Co}=280$ Å, and (c) $t_{Co}=600$ Å. The black arrows indicate the direction of the demagnetizing field applied before visualization.

A. Analysis of pattern roughening

Results of MFM experiments are shown in the left panels of Fig. 5 for three different Co film thicknesses. The patterns clearly change with film thickness, and for film thicknesses approaching 200 Å it was possible to observe a strong correlation of the stability of the parallel stripe domain pattern and the Co film thickness. Because the roughness of the films appears to be linked to film thickness, this motivated a study to see whether a correlation between film quality and the straightness of the domain boundary walls could be quantified.

The idea is to analyze a contrast image, such as that shown in the left panels of Fig. 5, using a two dimensional Fourier transform as shown in the right panels of the same figure. The transforms are represented by a gray scale image in a two dimensional plane with axes in units of spatial period. Results for three film thicknesses are shown: (a) $t_{Co}=200$ Å, (b) $t_{Co}=280$ Å, and (c) $t_{Co}=600$ Å. The black arrows indicate the direction of the demagnetizing field applied before visualization.

If the stripes were perfectly straight, parallel, and uniformly spaced, the Fourier transform would be sharply peaked at two points. The peaks would be located at posi-

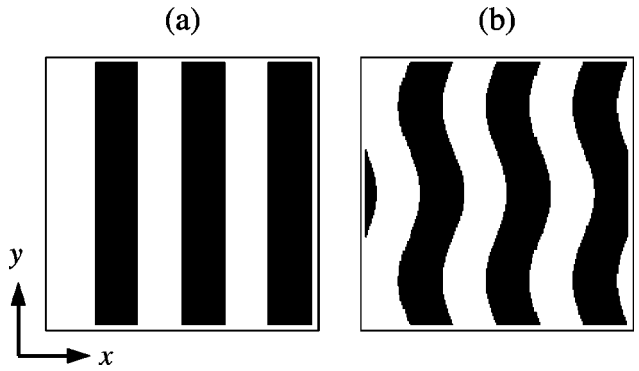

FIG. 6. Schematic diagram of a stripe pattern subject to imperfections: (a) The pattern is perfectly parallel and uniformly spaced. (b) Imperfections cause deviations in the stripe pattern. The spin orientation distribution is specified by the function $h(x,y)$ which is assigned $+1$ for the white areas and -1 for the black areas.

tions giving the spatial periods of the stripe array. The domain structures shown in Fig. 5 are far from parallel or straight, but there is a clear tendency towards improvement as the film thickness increases. Very regular and uniform parallel stripe arrays, with corresponding sharp peaks in period space, are in fact what were observed for the largest Co thickness samples.

The transforms in Fig. 5 show peaks distributed within a circle in period space, with the largest peaks contained in a ring of width 800 Å centered at a radius of 2000 Å. The transform gives a relatively simple way of quantifying the degree of wall straightness observed in the domain pattern. The angular distribution is measured by the angle subtended by a radius drawn from the center of the transform. An array with completely wandering walls, as shown in Fig. 5(a), produces instead a transform which subtends an angle of 180°.

To quantify this approach, consider the idealized perfect stripe domain pattern for a two dimensional array of Ising spins. A sketch is shown in Fig. 6(a). The spatial spin distribution is denoted by $h_0(x,y)$, where $h_0=1$ for ''up'' spins and $h_0=-1$ for ''down'' spins. With the addition of defects, the pattern may evolve into the equilibrium spin configuration depicted in Fig. 6(b). This spin distribution is denoted by $h(x,y)$.

The straightness of the stripe pattern is measured by a correlation function Δ for h defined by

$$\Delta \equiv \langle [h(x,y)-h_0(x,y)]^2 \rangle = \frac{1}{L^2}\int dxdy[h(x,y)^2+h_0(x,y)^2 - 2h_0(x,y)h(x,y)], \tag{1}$$

where L is the width of the square array of spins. Because this measures the deviation of the pattern from ideal straight parallel lines, the correlation function Δ is called the ''straightness parameter.'' Since $h(x,y)$ can only take on values of ± 1, then

$$\int dxdy h_0(x,y)^2 = \int dxdy h(x,y)^2 = L^2. \tag{2}$$

The cross-term $h_0(x,y)h(x,y)$ is only equal to -1 when there is a mismatch in the spin orientation at a particular site. Hence the total number of mismatches, δ, in a $L\times L$ array of spins satisfies

$$\int dxdy h_0(x,y)h(x,y) = L^2 - \delta. \tag{3}$$

It follows that

$$\Delta = \frac{2\delta}{L^2}. \tag{4}$$

The straightness parameter Δ in terms of the Fourier transformed spin distributions is

$$\Delta = \frac{1}{\sqrt{2\pi}L^2}\int dk_x dk_y [H(k_x,k_y)^2 + H_0(k_x,k_y)^2 - 2H(k_x,k_y)H_0^*(k_x,k_y)], \tag{5}$$

where $H(k_x,k_y)$ and $H_0(k_x,k_y)$ are the Fourier transforms of $h(x,y)$ and $h_0(x,y)$, respectively.

In Sec. IV, the correlation function Δ is calculated from numerical simulations using Eq. (5). Direct application of Eq. (5) to experimental data is complicated because (1) the ideal perfect stripe pattern is sample dependent and cannot be determined; and (2) the appropriate orientation of the stripe domains cannot be unambiguously determined. Any errors in either one of these points is magnified in Fourier space.

Instead, we obtain an estimate of the straightness of the stripe patterns from the angular spread of points in a Fourier transformed image as follows. The main contribution to the correlation function from Eq. (5) will come from the $H(k_x,k_y)^2$ and $H_0(k_x,k_y)^2$ terms because on average the cross terms will cancel. The $H_0(k_x,k_y)^2$ term represents the distribution for a perfect array and is therefore sharply peaked at two points in Fourier space and independent of roughness. The roughness dependent contribution will come from the $H(k_x,k_y)^2$ term.

If the main effect of roughness is to destroy the straightness of the domain stripes, as opposed to varying the width of the stripes, then $H(k_x,k_y)^2$ will contribute peaks along arcs containing the $H_0(k_x,k_y)^2$ points. If the $H_0(k_x,k_y)^2$ points lie a distance r away from the origin, then we can write $H(k_x,k_y)$ in polar coordinates, as

$$H(r,\theta)^2 = H_m \delta(r-r_k) \tag{6}$$

for $-\alpha \leq \theta \leq \alpha$, where $r^2=k_x^2+k_y^2$ and $\tan(\theta)=k_y/k_x$ as usual. The length r_k represents the radius of the distribution as measured on the FFT of the MFM image, and 2α measures the angular spread. In essence, we have approximated the distribution in the FFT image as a step function at a radius of r_k over an angular width of 2α, with a constant intensity of H_m. The integral of this term is

$$\int dk_x dk_y H(k_x,k_y)^2 = \int_0^\infty \int_{-\alpha}^{\alpha} H_m \delta(r-r_k) r\, d\theta\, dr = 2H_m r_k \alpha. \tag{7}$$

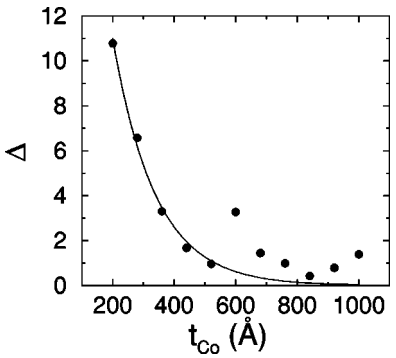

FIG. 7. Straightness parameter Δ versus nominal cobalt film thickness. Δ appears to decrease smoothly except near 600 Å, where a transition from perpendicular to partially in-plane occurs. The line of best fit shown is given by $\Delta = 46.43e^{-0.0072t_{\mathrm{Co}}}$. It is fitted to the first five data points.

Thus, the straightness parameter is proportional to the angular width of the points in the Fourier transformed MFM image.

B. Experimental results

This technique is used to examine the evolution of the domain pattern wall straightness as a function of Co film thickness. Examples were discussed in Fig. 5 where the MFM images and corresponding transforms are shown for three different Co film thicknesses. The subtended angle in the transform increases with decreasing Co film thickness. In each case a portion of a circular annulus is traced out, with a center radius measuring the mean period of the domain pattern and the radial width of the annulus segment providing information about the distribution of domain periodicities.

In Fig. 7, the straightness parameter Δ is plotted as a function of the nominal Co film thickness. The Δ appears to decrease smoothly with Co thickness except for two points near 600 Å. Except for these two points, the behavior for Co thicknesses approaching 200 Å from large thicknesses is fit best by an exponential function of the film thickness

$$\Delta \propto e^{-0.0072t_{\mathrm{Co}}}, \tag{8}$$

where t_{Co} is the thickness of the cobalt films.

Finally, we again note that the behavior above and below the film thickness of 600 Å may be due to changes in the domain magnetization orientation. The decrease in Δ from 200 Å to 520 Å is however due to the smoothing of the surface.

C. Numerical results

We attempt to provide a theoretical analysis of the data by numerical simulation of stripe domain formation. The simulation is based on representing competing ferromagnetic short range and dipolar long range interactions in an Ising model governed by the Hamiltonian

$$H = -\sum_{\langle i,j \rangle} J_{ij} S_i S_j + D \sum_{i,j} \frac{S_i S_j}{r_{ij}^3}. \tag{9}$$

Here J_{ij} is a nearest neighbor ferromagnetic exchange integral and the brackets $\langle i,j \rangle$ on the sum restrict the sum over nearest neighbors. r_{ij} is the distance between spins at sites i and j. The factor D measures the strength of the dipole interaction. The spins have a value of $+1$ or -1. A square array of 40×40 spins is considered and for computational efficiency, the dipole sums at a given location are restricted to include spins within a neighboring radius of 30 sites. Periodic boundary conditions are applied across all edges of the square array.

The stable stripe domain is determined by calculating the energy of patterns with different periodicities, and then choosing the periodicity that minimizes the energy. The relaxational dynamics are then determined in the following manner. The minimum energy stripe pattern is used as the initial configuration. A site is then chosen at random, and the orientation of the spin at that site is aligned in the direction of the local field h_i. The local field is

$$h_i = \sum_{\langle j \rangle} J_{ij} S_j - D \sum_j \frac{S_j}{r_{ij}^3}. \tag{10}$$

The process of aligning spins to the local field is repeated until a new stable equilibrium is reached. It is interesting to note that the dynamics can be very interesting in cases where the system is near a critical point where several metastable configurations exist nearby in energy. In such cases, there is a power law relationship between the total number of spin flips and the number of iterations required to reach an equilibrium. This type of behavior has been previously investigated in the context of self-organized criticality.[16]

The model was used to study the stability of the stripe domain with respect to perturbations in the exchange integrals J. This is accomplished by first establishing a stripe domain pattern, and then setting J to zero between some number of pairs of spins in two different types of simulation. In the first, ''defect'' sites were selected randomly, and in the second, a square perimeter of defects of length d was constructed. At a defect site, the exchange integral between neighboring spins is set to $J=0$. The relaxational dynamics are then followed until a new stable configuration forms. The straightness of the domain walls Δ is then calculated using Eq. (1) and studied as a function of the number N of zero J values introduced into the array.

An example of the first type of simulation is shown in Fig. 8(a) where the deterioration of a stripe pattern is followed for values of the number of random defects N between 10 and 200 for the 40×40 array of spins. The black squares represent spin down sites, and the white squares represent spin up sites. The figures depict four tiled arrays to emphasize the periodic boundary conditions imposed. The domain pattern appears to be robust to small numbers of N, but falls rapidly into a type of disorder for values of N greater than 100. This process was repeated 1000 times for each N value of zero J values in order to produce reasonable statistics on the domain wall straightness. Results of this numerical study are presented in Fig. 8(b). The plot in Fig. 8(b) is the straightness parameter Δ versus $1/N$ and can be fit by a power law of the form $\Delta \propto (1/N)^{-1.34}$.

In order to investigate whether any differences exist between randomly distributed zero J values and periodically

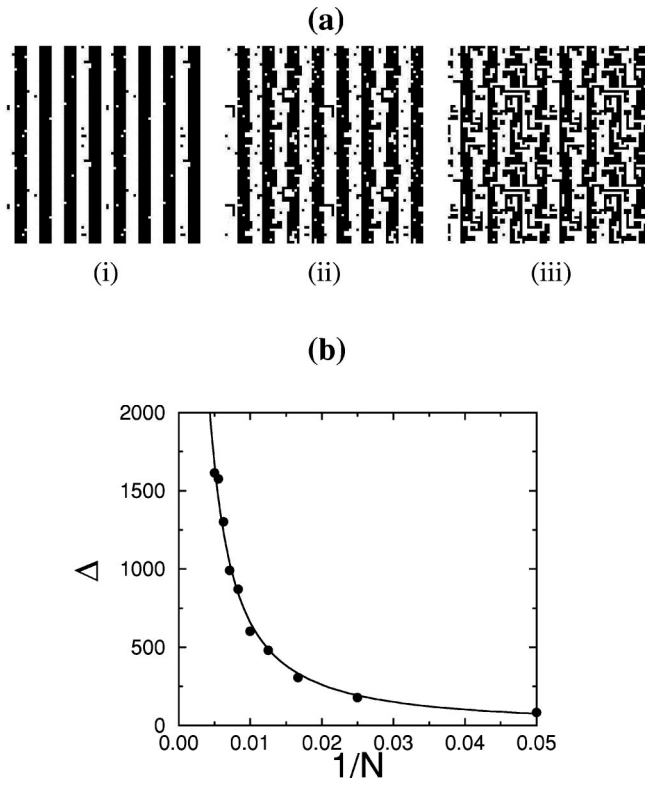

FIG. 8. (a) Equilibrium spin configurations calculated numerically in the presence of random defects, for $N=$ (i) 20, (ii) 100, and (iii) 200. (b) Straightness parameter Δ versus the reciprocal of the number of random defects, $1/N$. The line of best fit is given by $\Delta = 1.38(1/N)^{-1.34}$.

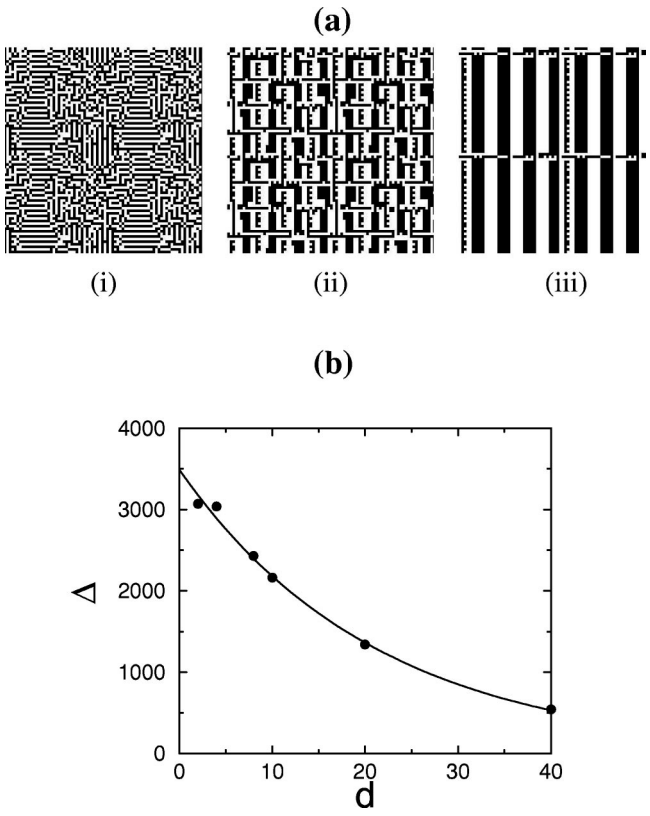

FIG. 9. (a) Equilibrium spin configurations calculated numerically in the presence of square defects, for $d=$ (i) 2, (ii) 10, and (iii) 40. (b) Straightness parameter Δ versus the square width, d. The line of best fit is given by $\Delta = 3490e^{-0.047d}$.

spaced zero J values, a second type of simulation was performed. In this case, the zero J values are placed along the perimeter of squares of width d, with the square edges parallel and perpendicular to the stripe pattern. The square defect is tiled such that neighboring squares share a common edge. In this regard, the simulation roughly approximates what one might expect at grain boundaries. Results of the square defects simulations are shown in Fig. 9. In Fig. 9(a), patterns for d between 2 and 40 are shown, and in Fig. 9(b), the corresponding deviations Δ are plotted against d. In this case, an exponential behavior is observed with the form being $\Delta \propto e^{-0.047d}$.

D. Discussion

A direct comparison of the model calculation results to experimental results is difficult. The model cannot represent such effects as weak in-plane orientation and finite wall widths that are clearly of some significance in the experimental Co system. However, the dynamics which we are attempting to probe should have some aspects that are not model specific. If the transition between continuous film behavior and island behavior does in fact affect the stability of the stripe domain pattern in a way analogous to a transition from an ordered configurational state, then some features of the transition near the critical point should be independent of many details of the model. In this system, the critical point is governed by a reduction of the near neighbor ferromagnetic exchange to a point where the exchange energy is comparable to the long range antiferromagnetic dipolar energy. This drives a transition between a kind of long range quasiferromagnetic order in the periodic stripe domain pattern, and a configuration dominated by a preference for antiparallel alignment. The straightness of the stripe domains is a measure of this competition, and in the real system is largely determined by the perpendicular components of the magnetization. Hence, an Ising like model of the kind used here should have relevance to the experimental situation.

The numerical simulations show that the approach to this critical point can be distinguished by the functional form of the straightness parameter Δ, which is sensitive to correlations in the placement of imperfections driving the transition. For the case of randomly placed imperfections, a power law behavior is observed with an exponent of 1.34. For the square defects, where the placement of the imperfections is strongly correlated, an exponential behavior is found. Whilst a comparison to the experimental behavior is questionable in terms of the difficulties involved in quantifying measures of the wall straightness and degree or imperfections or roughness, the experimentally data seemed to be best described by an exponential dependence as opposed to a power law fit. Because the film roughness seems to be due to islanding with a reasonably narrow distribution of island sizes, the corresponding behavior in the model should therefore be more like that of periodically placed defects rather than randomly placed defects. In this sense the experimental results appear to be in qualitative agreement with the numerical simulations.

IV. SUMMARY AND CONCLUSION

A model experimental system was studied in order to examine possible effects of thin film roughness on magnetic properties and domain pattern formation and stability. The system was constructed by depositing Co on islands of Ru. The resulting structure appeared to display properties typical of a continuous thin Co film together with properties characteristic of Co island formation. The relative importance of the two components could be varied by adjusting the Co film thickness.

Hysteresis curves were examined for Co film thicknesses that spanned the range between island and continuous film behavior. Consistent indications were found in the coercive fields, nucleation fields, saturation and remanence magnetization that two thickness regions exist. The thick film region, with thicknesses between 600 and 1000 Å, was essentially that of a correspondingly thick, smooth, thin film. The films with thicknesses below 600 Å showed indications of reduced nucleation, coercive and saturation fields consistent with an island dominated magnetic film. The thickness region around 600 Å was identified as the crossover region between structurally isolated islands and a connected island network interdispersed with deep valleys.

An interesting correlation between parallel stripe domain pattern stability and the degree of roughness was examined. A measure of the domain wall straightness was made using a Fourier transform of MFM images, and was found to correlate well with the Co film thickness. Numerical simulations were constructed, and examined for sensitivity to randomly and periodically placed imperfections in the exchange coupling. A transition away from straight parallel domain walls was also found and characterized by a power law behavior for randomly placed imperfections and an exponential behavior for periodically placed imperfections.

ACKNOWLEDGMENTS

K.O. and M.D. thank the Region Alsace No. 96/928/03/624 for support. R.L.S. and J.K. acknowledge support under the ARC. R.L.S. also thanks the CNRS for support. This work was partially supported by the EC-TMR program ''Dynaspin'' No. FMRX-CT97-0124.

*Present address: Unité PCPM, Université Catholique de Louvain, B-1348 Louvain-La-Neuve, Belgium.

[1] M. Seul and D. Andelman, Science **267**, 476 (1995).
[2] M. Seul and M. J. Sammon, Phys. Rev. Lett. **64**, 1903 (1990).
[3] R. E. Rosensweig, M. Zahn, and R. J. Shumovich, J. Magn. Magn. Mater. **39**, 127 (1983).
[4] J. A. Cape and G. W. Lehman, J. Appl. Phys. **42**, 5732 (1971).
[5] M. Seul and R. Wolfe, Phys. Rev. A **46**, 7519 (1992).
[6] M. Hehn, K. Ounadjela, S. Padovani, J.-P. Bucher, J. Arabski, N. Bardou, B. Bartenlian, C. Chappert, F. Rousseaux, D. Decanini, F. Carcenac, E. Cambril, and M.F. Ravet, J. Appl. Phys. **79**, 5068 (1996).
[7] P. Molho, J. L. Porteseil, Y. Souvhe, J. Gouzerh, and J. C. S. Levy, J. Appl. Phys. **61**, 4188 (1987).
[8] T. Garel and S. Doniach, Phys. Rev. B **26**, 325 (1982).
[9] M. Demand, M. Hehn, K. Ounadjela, Joo-Von Kim, A. V. Vagov, and R. L. Stamps, J. Appl. Phys. **85**, 5498 (1999).
[10] M. Hehn, S. Padovani, K. Ounadjela, and J. P. Bucher, Phys. Rev. B **54**, 3428 (1996).
[11] D. M. Donnet, K. M. Krishnan, and Y. Yajima, J. Phys. D **28**, 1942 (1995).
[12] M. Muller, J. Appl. Phys. **38**, 2413 (1967).
[13] A. A. Thiele, Bell Syst. Tech. J. **50**, 725 (1971).
[14] C. Kooy and U. Enz, Philips Res. Rep. **15**, 7 (1960).
[15] M. Demand, K. Ounadjela, Joo-Von Kim, R. L. Stamps, and M. Hehn (unpublished).
[16] X. Che and H. Suhl, Phys. Rev. B **44**, 155 (1991).